A Gravimetry-Based Fine Particle Concentration Measurement System for Humid Environment Using Graphene Oxide Layer

Budianto, Arif
Physics Study Program, University of Mataram

Wirawan, Rahadi
Physics Study Program, University of Mataram

Ramadian Ridho Illahi
Physics Study Program, University of Mataram

Dian Wijaya Kurniawidi
Physics Study Program, University of Mataram

他

https://doi.org/10.5109/7151690

出版情報：Evergreen. 10 (3), pp.1414-1421, 2023-09. 九州大学グリーンテクノロジー研究教育センター
バージョン：

A Gravimetry-Based Fine Particle Concentration Measurement System for Humid Environment Using Graphene Oxide Layer

Arif Budianto[1*], Rahadi Wirawan[1], Ramadian Ridho Illahi[1], Dian Wijaya Kurniawidi[1], Susi Rahayu[1], A.A. Ngurah Nara Kusuma[2], Alfina Taurida Alaydrus[1]

[1]Physics Study Program, University of Mataram, Mataram, Indonesia

[2]Biology Study Program, University of Mataram, Mataram, Indonesia

*Author to whom correspondence should be addressed:
E-mail: abudianto@unram.ac.id

(Received January 21, 2023; Revised August 25, 2023; accepted August 30, 2023).

Abstract: Recent studies have developed fine particle measurement systems using many methods. However, most of them are high-cost and unsuitable for harsh conditions. This study introduces a portable fine particle concentration system based on a gravimetry principle for air quality measurement in a highly humid environment. This study used a bare QCM (Q1) and graphene oxide-coated QCM (Q2) as the fine particle sensors. All sensors were installed inside a sensor box and tested at two different humidity levels: 75% (normal humidity) and 95% (high humidity). The sensors were tested using fine particle emissions (diameter 0.01 - 2.5 μm) emitted from several combustion sources (three biomass samples). A handheld particle concentration measurement device was used as the comparator for the measurement system. The results show that the uncoated QCM has a lower frequency response than the GO-coated QCM. The bare QCM does not show significant accuracy and linearity. As expected, the coated QCM performs better than the uncoated QCM, where the peak accuracies of the coated QCM are 98% and 99% for normal and high humidities. The linearity and sensitivity levels of the coated QCM are 95-99% and 0.59 – 1.76 Hz m^3 ug^{-1}. These performances confirm the reliability and ability of the developed system using GO layer and QCM to be employed as a fine particle emission sensing device in a humid environment.

Keywords: fine particle; gravimetry principle; graphene oxide; high humidity; quartz crystal microbalance

1. Introduction

Air pollution is related to emissions, a major green technology issue affecting everyone in many countries. Air pollution is also related to the emission sources, such as biomass burning[1,2)], industrial combustion process[3)], coal combustion[4–6)], and fuel combustion[7–9)]. These emissions are divided into particulate and gaseous emissions. Each classification has a different structure and chemical compounds depending on the emission sources. Gaseous emission can be found in carbon dioxide[10,11)], nitrogen dioxide, carbon monoxide, and many others[12)]. In terms of particulate emission or PM (particulate matter), it consists of solid particles and liquid droplets (both organic and inorganic compounds) suspended in the ambient air[8,13,14)].

PM emissions can be classified into two different distributions: particle number and particle mass distributions. PM is classified again into ultrafine, fine, coarse, and total suspended particles according to the average diameter. The smallest PM is an ultrafine particle or nanoparticle ($PM_{0.1}$; particles with aerodynamic diameter ≤ 0.1 μm)[8,15)]. Fine particle or $PM_{2.5}$ has an average diameter of < 2.5 μm[16,17)]. Coarse particle (PM_{10}) has a bigger diameter than ultrafine and fine particles, with an aerodynamic diameter ≤ 10 μm[18)].

Exposure to PM in certain concentrations decreases the air quality index and health quality. PM has a high association with PM penetration inside the body system. They might penetrate alveoli and deposit to the alveolar surface area[19)]. They follow the bloodstream and harm the lungs[20)], brains[21)], and erythrocytes[22)].

PM concentration measurement is a mitigation system to monitor and decrease PM concentration. Many techniques are applied to measure PM concentration, such as a fast spectrometer (such as a scanning mobility particle sizer)[23,24)], a low-pressure impactor[8)], and a light scattering method[25,26)]. A light scattering method has good

sensitivity and can detect a single particle using a laser beam and a photo-detector (in the unit of particle number). A previous study showed a fine particle measurement system using a virtual impactor and a surface acoustic wave (SAW), which has good repeatability and accuracy. This system performs well with a sensitivity of 7.446 Hz/min per μg/m^3 [27]. It can be determined that the existing methods or principles indeed have high sensitivity, fast response time, and high accuracy. However, they can be categorized as high-cost devices. Most cannot be used in harsh conditions, such as in a high-humidity environment (humidity >80%). There will be a serious problem in the sensing part regarding the high moisture content in the surrounding area. They also need specific terms, such as room condition (controlled room temperature, dust-free area, and indoor-used only) and trained operators.

QCM (quartz crystal microbalance) is a crystal with an actuator-sensor characteristic. This crystal has a gravimetry principle with a fluctuating resonance frequency related to the deposited mass onto its electrode surface. A gravimetry principle shows that the deposited mass is linearly correlated with the frequency shift[28]. That is why many studies introduce the QCM performance in different treatments, such as a gas sensor[28]. QCM is a mass-sensitive sensor when it has a selective layer on its surface[29].

Graphene oxide (GO) is a derivative product of carbon. GO has large surface areas (hydrophilic surface area) and is reach of hydrophilic functional groups[30–32]. GO has good mechanical modulus that makes it suitable for QCM layer (a small probability of the swelling effect)[33]. In terms of QCM layer, GO has been applied as sensitive layers for gas detections[34,35].

Based on the introduction, a fine particle monitoring system should be useable in certain conditions. Though there has been a tremendous improvement in monitoring fine particle concentration, it is interesting to ask what is the stability and durability of the monitoring system in response to the temporal and different environmental conditions, especially the issues in an extreme environment with high humidity. Following the QCM characteristic and measurement needs, this study aims to develop a novel particulate concentration measurement system for a high-humidity environment using a QCM crystal as the sensor. For this purpose, this study used a GO layer as a sensitive thin film to bind fine particles as air pollution. GO was chosen due to its unique characteristics, such as being hydrophilic, easy to use as a coating material, large surface area, and many others. This research introduces a novel particulate measurement system, providing a low-cost method that performs well in harsh conditions.

2. Materials and methods

2.1 Developed system

The measurement system was developed using QCM sensors (base frequency f_0 = 4.998 MHz, electrode area A = 0.196 cm^2): Q1 and Q2. Q1 sensor was not coated (silver electrodes, Ag). Q2 was coated using a graphene oxide (purity = 99%, single layer, volume = 0.05 ml, concentration = 2 mg/ml) layer with a spin coating method (rotation = 700 RPM). All sensors were connected to a suction pump ((flow-rate = 2 m/s) and a driver consisting of an oscillator and a frequency counter (Fig. 1). The oscillator was used to drive and trigger the QCMs. In contrast, the QCM's frequency outputs were measured using the frequency counter.

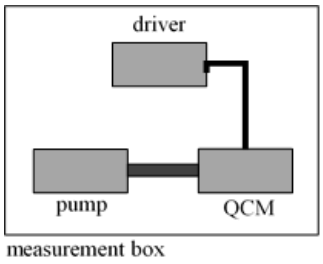

Fig. 1: The schematic of the developed system inside a measurement box.

2.2 Fine particle generation

This study used three emission sources (biomass samples) for fine particle generation: C_1 (corn cob), C_2 (tobacco leaves), and C_3 (rice husk). The samples were selected randomly to identify the measurement system's performance. Each sample was weighed to control the mass (m_0) for the measurement repetition (n = 3 repeated measurements), then burnt inside a furnace to generate emission. The produced emission was pumped into an experimental chamber (via input probe) made from the acrylic board (V = 12,000 cm^3) connected to a suction pump (flow-rate = 2 m/s) and filter paper (a Whatman filter paper, Grade = 5). The suction pump and filter paper were used to block bigger particles and only let particles with a diameter ≤2.5 μm (fine particle)[36].

This study used two conditions for each biomass sample: A (humidity = 75%, normal humidity) and B (humidity = 95%, high humidity) to identify the influence of humidity and the measurement result. The humidity inside the chamber was set and controlled using a humidifier device filled with pure water in different humidification durations: 20 s (A, low humidity) and 40s (B, high humidity). According to a preliminary experiment, these humidification durations were selected to obtain the selected humidity condition.

2.3 Fine particle measurement

The developed system and a comparator device (Hinaway, model CW-HAT200s) were used to measure fine particle concentrations inside the experimental

chamber before and after exposure via the outlet probe. The measurements were conducted for 300 s with a sampling time of 10 s. The measurement aimed to obtain the fine particle concentration from the device (C_c) and comparator (C_m) related to the system's performance calculation, including accuracy (A), linearity (r), sensitivity (S), and measurement range. This duration (300 s) was selected according to the preliminary experiment since the measurement time >300 s has no fine particle concentration anymore. This treatment was conducted for A and B conditions using all samples (Fig. 2).

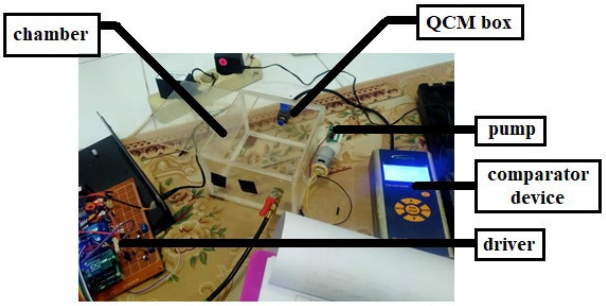

Fig. 2: The schematic design of fine particle concentration measurement.

2.4 Statistical analysis

Based on the measured frequency shift (Δf, output of the frequency counter), the fine particle mass (Δm) is calculated using Eq. 1 (Sauerbrey's equation).

$$\Delta m = - \frac{A\sqrt{\rho\,\mu}}{2 f_0^2} . \Delta f \qquad (1)$$

The constants of μ and ρ are shear modulus (2.947×10^{11} g/cm.s^2) and crystal density (2.684 g/cm^3). The device concentration (C_c) was calculated using Eq. 2[25]:

$$C_c = \frac{\Delta m}{V} \qquad (2)$$

All results were interpreted as the mean value and standard deviation. A linear equation was used to approach the data trendline, while the performance data were shown by the regression coefficient (R^2) and the linearity percentage (r). $R^2 > 0.90$ was determined as significantly correlated. The data significance was analyzed also using a t-test[37].

The accuracy A was calculated by comparing the values from the measured and calculated data (ΔC) with the comparator values C_m. The sensitivity level (S) was determined by comparing the output frequency shift (Δf) with the series of fine particle concentrations from the comparator (C_m), Eq. 3[38].

$$S = \frac{\Delta f}{C_m} \qquad (3)$$

3. Results and Discussion

3.1 Measured fine particle

This measurement was conducted to obtain the comparator value from a laboratory-calibrated device. The resulting data is determined as the measured concentration, C_m. According to the result under 300 s measurement time (t), the total fine particle concentration ranges from 2,398 μg/m^3 to 8,401 μg/m^3 (Table 1). C_1 from the corn cob sample has the highest concentration: 6,528 μg/m^3 (A) and 8,401 μg/m^3 (B).

As seen in Table. 1, the second position belongs to the C_2 sample, resulting in 2,706 μg/m^3 (A) and 4,512 μg/m^3 (B). The difference between normal and high humidities is up to 1,800 μg/m^3. These results are followed by the last sample, C_3, in the 3rd position (determined as the cleanest source compared to other samples).

According to the results, the calculated fine particle mass is up to 40 μg, which can be categorized as a microgram scale. These results confirm a significant difference in fine particle concentrations between low and high humidity levels measured by the comparator. Higher humidity has a higher fine particle concentration.

The results show that the samples (biomass burning) emitted fine particles in different concentrations, where rice husk is the cleanest. As confirmed by a previous study concerning particulate matter's impact on health, each biomass has a different emission factor[39]. The emission factor influences the produces particulate matter. The previous study shows corn cob has higher emissions than tobacco leaves and rice husks[22].

Table 1. Fine particle concentrations from the comparator.

Fine Particle Concentrations (μg/m^3)		
Samples	**A**	**B**
C_1	6528	8401
C_2	2706	4512
C_3	2398	2721
Fine Particle Mass (μg)		
C_1	111	142
C_2	46	77
C_3	41	46

3.2 Frequency responses

The developed system was tested to identify the frequency response due to the fine particle exposure inside the exposure chamber (Fig. 3a-b). At the first peak on the normal humidity measurement (Fig. 3), a significant difference exists between Q1 and Q2. In the case of Q1 (a bare QCM sensor), the frequency shifts fluctuate. The highest frequency shifts of Q1 are 100 Hz, 85 Hz, and 60 Hz, respectively, for C_1, C_2, and C_3. Besides, in Q2, C_1 (determined as the dirtiest emission source in this study) has 310 – 330 Hz of frequency shift, while C_2 has only 105 – 130 Hz of frequency shift (the 2nd position). The

difference between them is more than 200 Hz indicating a better response from the C_1 sample (since C_1 has more fine particle concentrations). The increasing trendline can be seen in the next peaks, in which the frequency shift of the C_1 sample on the last peak is 840 – 870 Hz. C_3, the cleanest one, has the smallest frequency shift than C_1 and C_2. C_3 only has 40 – 110 Hz of frequency shift. According to these results, it can be seen that Q2 has a better frequency shift than Q1 in condition-A (normal humidity).

In the high humidity measurement, Q1 has low responses, indicated by the maximum frequency shift of 95 Hz (C_1). C_2 and C_3 have the maximum frequency shifts of 90 Hz and 95 Hz. Q1 does not significantly differ in measuring C_1, C_2, and C_3. In contrast, the frequency response due to the fine particle exposure is higher than in the low humidity measurement (Fig. 3b). C_3 shows a frequency shift of 15 – 155 Hz. Compared to condition-A, condition B has more responses indicating a better sensing ability. A similar result is obtained at C_2, which is higher (210 – 400 Hz) than the low humidity measurement. As expected, C_1 has the highest response among all variations, resulting in 450 – 1,135 Hz of the frequency shift.

Based on the fine particle mass in Table 1, the most mass is obtained at C_1 in all humidity conditions. As expected, Q1 does not interpret a similar trendline with the humidity conditions since the frequency responses fluctuate. Meanwhile, Q2 shows better responses since the highest frequency shift is also obtained at the high humidity condition (B). These results follow Sauerbrey's equation, where more deposited mass on the QCM's surface generates a higher frequency response[40].

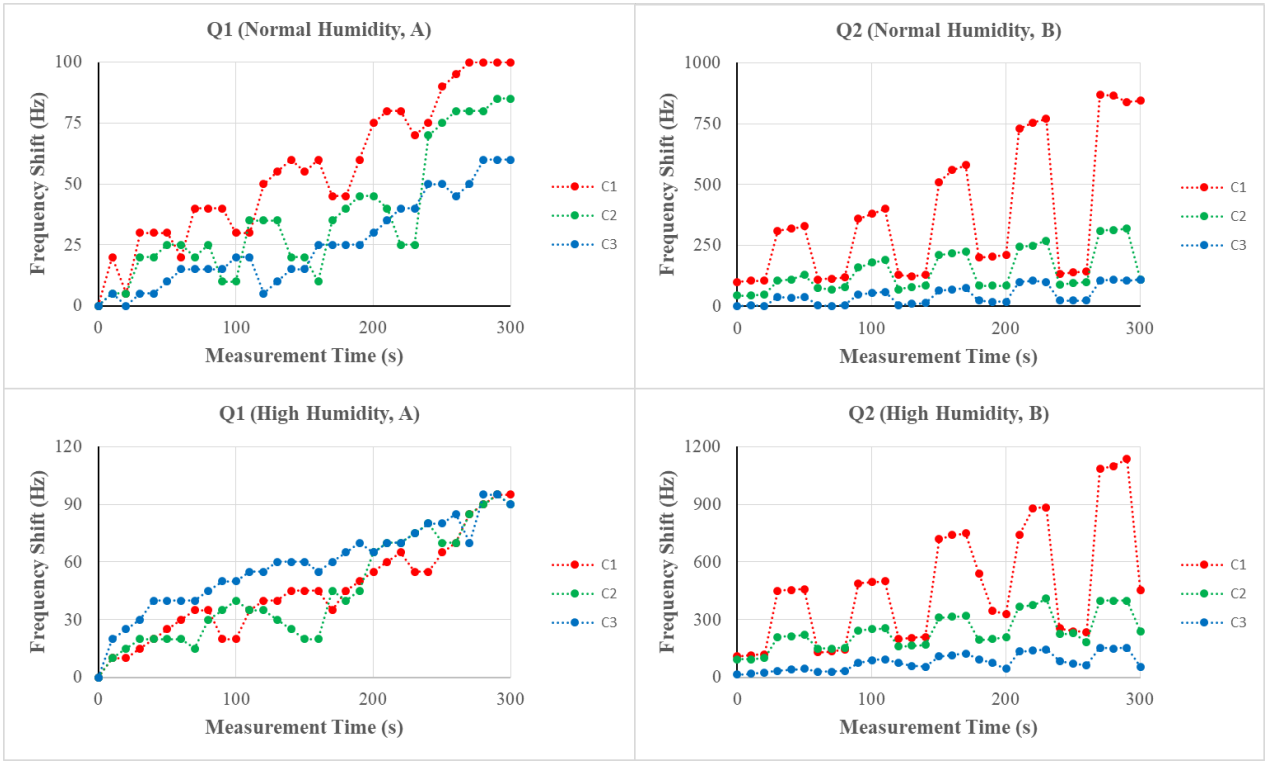

Fig. 3. Measured frequency for the low and high humidity measurements for both Q1 and Q2.

3.3 Accuracy, linearity, and sensitivity levels

Table 2 shows the calculated fine concentrations for normal and high humidity conditions.

Table 2. The comparison of accuracy levels between the uncoated QCM (Q1) and GO-coated QCM (Q2).

Samples	Concentrations (µg/m^3)		*A* (%)	
	Q1	Q2	Q1	Q2
Normal Humidity (A)				
C_1	994	6682	15	98
C_2	657	2609	24	96
C_3	459	819	19	34
High Humidity (B)				
C_1	808	8515	10	99
C_2	802	4311	18	96
C_3	1043	1421	38	52

Table 2 shows that Q2 has low accuracy. The best accuracy is only 38% obtained at C_3. In condition-A, the accuracy levels of Q1 are ranging from 15-24%. In condition B, the accuracy levels somehow decrease but also increase. The resulting data does not interpret a trendline.

In contrast, Q2 sensors from C_1 and C_2 measurements have good accuracy levels for both normal (A) and high

humidities (B). The accuracy levels are >90%. The developed system works well in sensing or detecting fine particle concentrations in both normal and harsh conditions (humid environments). In contrast, C_3 has a lesser accuracy, with values of <60% for both high and normal conditions. It might be related to the biomass sample characteristic of rice husk that needs further investigation and explanation.

Figure 4 interprets the linearity test results for all humidity variations. The linearity data shows that all measurement results have R^2 values of >0.95. It can be determined that the developed system has good linearity (95% to 99%) for sensing fine particles from biomass samples. No significant difference exists between high and normal humidity conditions ($p = 0.82$). In other words, in terms of linearity, the developed system works well in measuring fine particle concentration for both normal and high humidity levels.

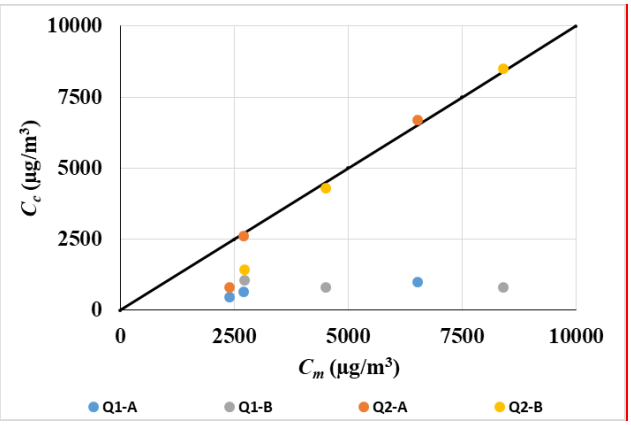

Fig. 4: Linearity levels.

The sensitivity levels are interpreted in Table 3. Interestingly for Q2, the sensitivity levels of conditions A and B are statistically similar. The sensitivity levels are > 1 Hz.m^3/µg for C_1 and C_2. C_3 is not quietly sensitive to use in normal and humid conditions. As expected, Q1 has the lowest sensitivity level. All sensitivity levels are < 1 Hz.m^3/µg.

Table 3. Sensitivity levels of the developed system device.

Sensitivity of Q1 (Hz.m^3/µg)		
Samples	**A**	**B**
C_1	0.26	0.17
C_2	0.42	0.31
C_3	0.33	0.66
Sensitivity of Q2 (Hz.m^3/µg)		
Samples	**A**	**B**
C_1	1.76	1.74
C_2	1.66	1.64
C_3	0.59	0.90

The resulting data show that the developed system using a QCM sensor has good linearity, sensitivity, and accuracy levels, especially for the corn cob and tobacco leaves samples. The results are related to the unique principle of a QCM sensor for gravimetric measurements. As interpreted in Table 1, all samples have specific fine particle masses that might interact and be deposited on the sensor. As confirmed by a previous study, QCM works by a gravimetry principle related to the frequency shift and mass loading effect[41,42]. QCM has a fundamental frequency of f_0, while the frequency shift Δf is linear to the deposited mass on the crystal surface[29]. Generally, a QCM is a microbalance, where more deposited masses reflect more frequency shifts[43].

The developed system's ability and calculated performances are well related to the interaction between the deposited mass and QCM's surface. As supported by a previous study, QCM's performance is influenced by many factors, including the coating material applied to the surface area (A)[43]. A selective and sensitive coating material will have high physical or other bindings[28,44]. That is why this study used a graphene oxide-coated QCM. GO plays an important role in the humidity influence since it has a high specific surface area and good hydrophilicity[45]. As a hydrophilic material, GO is not a water-resist material, making it suitable for humidity sensing.

The important role is the GO layer as the selective material. GO and several graphene-based sensitive layers have extremely high surface-to-volume ratios, with many atoms exposed to the surrounding environment[46]. Regarding hydrophilic and hydrophobic characteristics, GO sheets are highly soluble in water due to the existence of oxygen functional groups. GO also has a sp_2 network that generates p-p interactions with the aromatic substances and conjugated polymers[47]. This interaction may cause a sensitive layer interaction for a humid molecule due to the adsorbed–desorbed masses of water molecule[48]. In a low humid condition, the GO layer-based QCM carboxyl groups have high adsorbed – desorbed water molecules on their external carbon surface. Interestingly, the internal stress of the GO layer is not affected in the low-humid condition[46]. Besides, the change of QCM energy related to the H-bonding (from water molecule) and C-OH possibly influences the crystal performance in a high-humidity environment. A previous study states that C-O groups from the GO layers (as the water molecules) enter the carbon interlayer and generate a large interlayer expansion of GO layers[48]. That is why, in a highly humid environment (as condition B in this study), the GO layer may have more internal stress regarding the GO expansion, making the sensor have a higher frequency shift than in lower humidity. In other words, it can be assumed that the QCM performances are indeed influenced by the adsorbed-desorbed water molecules and the GO expansion. The counted frequency shifts are observed until the crystal reaches the saturated

value due to the swelling effect. Compared to a bare sensor (Q1), GO in Q2 also has a good mechanical modulus which may cause a small probability of the swelling effect (the most problem found in a QCM application) due to the over-mass loading impact. In other words, GO can overcome false readings regarding the moisture content or over-deposited mass) that influences the QCM response[33].

A non-significant result is observed in the rice husk sample. This sample has the lowest accuracy for normal and high humidity conditions (34-52%). These results may correlate with rice husks' chemical compounds and physical characteristics. According to a previous study, rice husk has alkali metal content[49]. These components might block the QCM's surface, generating coarse fiber and influencing the interaction between GO and particles.

4. Conclusion

The developed system works well in detecting fine particle concentration for both normal and high humidity levels indicated by good linearity level (>90%). The accuracy level is >90% for corn cob and tobacco leave measurements, with a> 1 Hz.m3/µg sensitivity. The system performs less in detecting fine particles from rice husk burning emission since the accuracy is <60% (sensitivity <1 Hz.m^3/µg).

This study may be useful as a preliminary study for developing an aerosol measurement system in a better performance, especially in a harsh environment. The developed system can be integrated with other sensitive layer for further investigations to obtain a better sensitivity. The developed system is easy to be developed with other thin films using a standard principle.

Acknowledgments

All authors wish to acknowledge the kind hands of Adinda Kartika Sari and Ummi Amanah (from the University of Brawijaya, Malang, Indonesia).

Nomenclature

A	Area (m^2)
C_c	Calculated concentration (µg/m^3)
C_m	Measured concentration (µg/m^3)
f_0	Fundamental frequency (Hz)
Δf	Frequency shift (Hz)
R^2	Regression coefficient
r	Linearity (%)
S	Sensitivity (Hz m^3/µg)

References

1) T. Sitek, J. Pospíšil, J. Poláčik, M. Špiláček, and P. Varbanov, "Fine combustion particles released during combustion of unit mass of beechwood," Renew. Energy, **140** 390–396 (2019). doi:10.1016/j.renene. 2019.03.089.
2) Y. Furutani, K. Norinaga, S. Kudo, J.I. Hayashi, and T. Watanabe, "Current situation and future scope of biomass gasification in Japan," Evergreen, **4**(4) 24–29 (2017). doi:10.5109/1929681.
3) J. Mertens, H. Lepaumier, P. Rogiers, D. Desagher, L. Goossens, A. Duterque, E. Le Cadre, M. Zarea, J. Blondeau, and M. Webber, "Fine and ultrafine particle number and size measurements from industrial combustion processes: primary emissions field data," Atmos. Pollut. Res., **11** (4) 803–814 (2020). doi:10.1016/j.apr.2020.01.008.
4) D. Khatri, A. Gopan, Z. Yang, A. Adeosun, and R.L. Axelbaum, "Characterizing early stage sub-micron particle formation during pulverized coal combustion in a flat flame burner," Fuel, **258** (May) 115995 (2019). doi:10.1016/j.fuel.2019.115995.
5) P.S. Oetari, S.P. Hadi, and H.S. Huboyo, "Trace elements in fine and coarse particles emitted from coal-fired power plants with different air pollution control systems," J. Environ. Manage., **250** 109497 (2019). doi:10.1016/j.jenvman. 2019.109497.
6) A. Saiful, A.T. Wijayanta, K. Nakaso, and J. Fukai, "Predictions of O_2/N_2 and O_2/CO_2 mixture effects during coal combustion using probability density function," Evergreen, **2** 12–16 (2010).
7) C.H. Jeong, A. Traub, and G.J. Evans, "Exposure to ultrafine particles and black carbon in diesel-powered commuter trains," Atmos. Environ., **155** 46–52 (2017). doi:10.1016/j.atmosenv.2017.02. 015.
8) Y. Fujitani, K. Takahashi, A. Fushimi, S. Hasegawa, Y. Kondo, K. Tanabe, and S. Kobayashi, "Particle number emission factors from diesel trucks at a traffic intersection: long-term trend and relation to particle mass-based emission regulation," Atmos. Environ. X, **5** 100055 (2020). doi:10.1016/j.aeaoa.2019.100055.
9) D.A. Sugeng, W.J. Yahya, A.M. Ithnin, B.H. Kusdi, M.A.A. Rashid, I. Bahiuddin, N.A. Mazlan, and H.A. Kadir, "Experimental comparison of smoke opacity and particulate matter emissions with the use of emulsion fuel," Evergreen, **7**(3) 452–457 (2020). doi.org:10.5109/4068626
10) N.A. Lestari, "Reduction of CO_2 emission by integrated biomass gasification-solid oxide fuel cell combined with heat recovery and in-situ co2 utilization," Evergreen, **6**(3) 254–261 (2019). doi:10.5109/2349302.
11) M.H. Huzaifi, M.A. Budiyanto, and S.J. Sirait, "Study on the carbon emission evaluation in a container port based on energy consumption data," Evergreen, **7**(1) 97–103 (2020). doi:10.5109/ 2740964.
12) S. Abikusna, B. Sugiarto, and I. Yamin, "Utilization analysis of bioethanol (low grade) and oxygenated additive to cov and gas emissions on si engine,"

Evergreen, **7**(1) 43–50 (2020). doi:10.5109/2740940.
13) M.K. Verma, L.K.S. Chauhan, S. Sultana, and S. Kumar, "The traffic linked urban ambient air superfine and ultrafine PM_1 mass concentration, contents of pro-oxidant chemicals, and their seasonal drifts in lucknow, India," Atmos. Pollut. Res., **5** (4) 677–685 (2014). doi:10.5094/APR.2014.077.
14) V. V Chernyshev, A.M. Zakharenko, S.M. Ugay, T.T. Hien, L.H. Hai, S.M. Olesik, A.S. Kholodov, E. Zubko, M. Kokkinakis, T.I. Burykina, A.K. Stratidakis, and Y.O. Mezhuev, "Morphological and chemical composition of particulate matter in buses exhaust," Toxicol. Reports, **6** (December 2018) 120–125 (2019). doi:10.1016/j.toxrep. 2018.12.002.
15) M. Geiser, T. Stoeger, M. Casaulta, S. Chen, M. Semmler-behnke, I. Bolle, S. Takenaka, W.G. Kreyling, and H. Schulz, "Biokinetics of nanoparticles and susceptibility to particulate exposure in a murine model of cystic fibrosis," 1–15 (2014).
16) Y. Xie, O.A. Fajardo, W. Yan, B. Zhao, and J. Jiang, "Six-day measurement of size-resolved indoor fluorescent bioaerosols of outdoor origin in an office," Particuology, **31** 161–169 (2017). doi:10.1016/j.partic.2016.09.004.
17) B. Feenstra, V. Papapostolou, S. Hasheminassab, H. Zhang, B. Der Boghossian, D. Cocker, and A. Polidori, "Performance evaluation of twelve low-cost PM2.5 sensors at an ambient air monitoring site," Atmos. Environ., **216** 116946 (2019). doi:10.1016/j.atmosenv.2019.116946.
18) M. Eeftens, H.C. Phuleria, R. Meier, I. Aguilera, E. Corradi, M. Davey, R. Ducret-Stich, M. Fierz, R. Gehrig, A. Ineichen, D. Keidel, N. Probst-Hensch, M.S. Ragettli, C. Schindler, N. Künzli, and M.-Y. Tsai, "Spatial and temporal variability of ultrafine particles, NO_2, $PM_{2.5}$, $PM_{2.5}$ absorbance, PM_{10} and PM_{coarse} in swiss study areas," Atmos. Environ., **111** (2) 60–70 (2015). doi:10.1016/j.atmosenv.2015.03.031.
19) G. Buonanno, L. Stabile, and L. Morawska, "Personal exposure to ultrafine particles: the influence of time-activity patterns," Sci. Total Environ., **468–469** 903–907 (2014). doi:10.1016/j.scitotenv.2013.09.016.
20) G. Buonanno, G. Giovinco, L. Morawska, and L. Stabile, "Lung cancer risk of airborne particles for italian population," Environ. Res., **142** 443–451 (2015). doi:10.1016/j.envres.2015.07.019.
21) J.L. Allen, X. Liu, D. Weston, K. Conrad, G. Oberdörster, and D.A. Cory-Slechta, "Consequences of developmental exposure to concentrated ambient ultrafine particle air pollution combined with the adult paraquat and maneb model of the parkinson's disease phenotype in male mice," Neurotoxicology, **41** 80–88 (2014). doi:10.1016/j.neuro.2014.01.004.
22) K. Al Hadi, A.Y.P. Wardoyo, U.P. Juswono, A. Naba, A. Budianto, and E.T.P. Adi, "A study of erythrocyte deformation level related to biomass burning emission exposures using artificial neural networks," Polish J. Environ. Stud., **31** (6) 5037–5046 (2022). doi:10.15244/pjoes/150643.
23) M. Masiol, S. Squizzato, D.C. Chalupa, M.J. Utell, D.Q. Rich, and P.K. Hopke, "Long-term trends in submicron particle concentrations in a metropolitan area of the northeastern united states," Sci. Total Environ., **633** 59–70 (2018). doi:10.1016/j.scitotenv.2018.03.151.
24) Z. Németh, B. Rosati, N. Zíková, I. Salma, L. Bozó, C. Dameto de España, J. Schwarz, V. Ždímal, and A. Wonaschütz, "Comparison of atmospheric new particle formation events in three central european cities," Atmos. Environ., **178** 191–197 (2018). doi:10.1016/j.atmosenv. 2018.01.035.
25) A. Budianto, A.Y.P. Wardoyo, M. Masruroh, H.A. Dharmawan, and M. Nurhuda, "Performance test of an aerosol concentration measurement system based on quartz crystal microbalance performance test of an aerosol concentration measurement system based on quartz crystal microbalance," J. Phys. Conf. Ser., **1811** 1–8 (2021). doi:10.1088/1742-6596/1811/1/012033.
26) A. Wardoyo, and A. Budianto, "A dc low electrostatic filtering system for pm2.5 motorcycle emission," IEEE Xplore, **1** 51–54 (2017).
27) Y. Wang, Y. Wang, W. Liu, D. Chen, C. Wu, and J. Xie, "An aerosol sensor for pm1 concentration detection based on 3D printed virtual impactor and saw sensor," Sensors Actuators, A Phys., **288** 67–74 (2019). doi:10.1016/j.sna.2019.01.013.
28) I.R. Jang, S.I. Jung, G. Lee, I. Park, S.B. Kim, and H.J. Kim, "Quartz crystal microbalance with thermally-controlled surface adhesion for an efficient fine dust collection and sensing," J. Hazard. Mater., **424** (B) 127560 (2022). doi:https://doi.org/10.1016/j.jhazmat.2021.127560.
29) N. Liu, X. Xiang, M. Sun, P. Li, H. Qin, H. Liu, Y. Zhou, L. Wang, L. Wu, and J. Zhu, "Flexible hydrogel non-enzymatic qcm sensor for continuous glucose monitoring," Biosens. Bioelectron. X, **10** 100110 (2022). doi:10.1016/j.biosx.2022.100110.
30) D. Zhang, X. Song, Z. Wang, and H. Chen, "Ultra-highly sensitive humidity sensing by polydopamine/graphene oxide nanostructure on quartz crystal microbalance," Appl. Surf. Sci., **538** 147816 (2021). doi:10.1016/j.apsusc.2020. 147816.
31) E. Kusrini, F. Oktavianto, A. Usman, D.P. Mawarni, and M.I. Alhamid, "Synthesis, characterization, and performance of graphene oxide and phosphorylated graphene oxide as additive in water-based drilling fluids," Appl. Surf. Sci., **506** 145005 (2020). doi:10.1016/j.apsusc. 2019.145005.
32) E. Kusrini, A. Suhrowati, A. Usman, M. Khalil, and V. Degirmenci, "Synthesis and characterization of graphite oxide, graphene oxide, and reduced graphene oxide from graphite waste using modified

hummers' method and zinc as reducing agent," Int. J. Technol., **10** (6) 1093–1104 (2019). doi:10.14716/ijtech.v10i6.3639.

33) C.Y. Ho, and Y.S. Wu, "Diamine decorated graphene oxide film on quartz crystal microbalance for humidity-sensing analysis," Appl. Surf. Sci., **510** 145257 (2020). doi:10.1016/j.apsusc.2020.145257.
34) M. Yang, and J. He, "Graphene oxide as quartz crystal microbalance sensing layers for detection of formaldehyde," Sensors Actuators, B Chem., **228** 486–490 (2016). doi:10.1016/j.snb.2016. 01.046.
35) S. Jayawardena, A. Kubono, R.M.G. Rajapakse, and M. Shimomura, "Effect of titanium precursors used in the preparation of graphene oxide/TiO2 composite for gas sensing utilizing quartz crystal microbalance," Nano-Structures & Nano-Objects, **28** 100780 (2021). doi:10.1016/j.nanoso. 2021.100780.
36) A.Y.P. Wardoyo, U.P. Juswono, and J.A.E. Noor, "The association between the diesel exhaust particle exposure from bus emission and the tubular epithelial cell deformation of rats," Environ. Sci. Pollut. Res., **27** (18) 23073–23080 (2020). doi:10.1007/s11356-020-08752-x.
37) V.C. Waila, A. Sharma, and M. Yusuf, "Optimizing the performance of solar pv water pump by using response surface methodology," Evergreen, **9**(4) 1151–1159 (2022). doi.org:10.5109/6625726
38) A. Budianto, A.Y.P Wardoyo, Masruroh, and H.A. Dharmawan, "An airborne fungal spore mass measurement system based on graphene oxide coated QCM," Polish J. Environ. Stud., **31** (4) 1–7 (2022). doi:10.15244/pjoes/147057.
39) A.Y.P. Wardoyo, L. Morawska, Z.D. Ristovski, M. Jamriska, S. Carr, and G. Johnson, "Size distribution of particles emitted from grass fires in the northern territory, australia," Atmos. Environ., **41** (38) 8609–8619 (2007). doi:10.1016/j.atmosenv.2007.07.020.
40) S. Jayawardena, H.D. Siriwardena, R.M.G. Rajapakse, A. Kubono, and M. Shimomura, "Fabrication of a quartz crystal microbalance sensor based on graphene oxide/tio2 composite for the detection of chemical vapors at room temperature," Appl. Surf. Sci., 493 (June) 250–260 (2019). doi:10.1016/j.apsusc.2019.06.280.
41) R. Yi, B. Peng, Y. Zhao, D. Nie, L. Chen, and L. Zhang, "Quartz crystal microbalance humidity sensors based on structured graphene oxide membranes with magnesium ions: design, mechanism and performance," Membranes (Basel)., **12** 125 (2022). doi:https://doi.org/10.3390/membranes12020125.
42) M. Yılmaz, M. Bakhshpour, I. Göktürk, A.K. Pişkin, and A. Denizli, "Quartz crystal microbalance (QCM) based biosensor functionalized by her2/neu antibody for breast cancer cell detection," Chemosensors, **9** (4) (2021). doi:10.3390/chemosensors9040080.
43) C.E. Kirimli, E. Elgun, and U. Unal, "Machine learning approach to optimization of parameters for impedance measurements of quartz crystal microbalance to improve limit of detection," Biosens. Bioelectron. X, **10** 100121 (2022). doi:10.1016/j.biosx.2022.100121.
44) T. Liangsupree, E. Multia, P. Forssén, T. Fornstedt, and M.-L. Riekkola, "Kinetics and interaction studies of anti-tetraspanin antibodies and icam-1 with extracellular vesicle subpopulations using continuous flow quartz crystal microbalance biosensor," Biosens. Bioelectron., **206** 114151 (2022). doi:10.1016/j.bios.2022.114151.
45) H.Y. Mohammed, M.A. Farea, P.W. Sayyad, N.N. Ingle, T. Al-Gahouari, M.M. Mahadik, G.A. Bodkhe, S.M. Shirsat, and M.D. Shirsat, "Selective and sensitive chemiresistive sensors based on polyaniline/graphene oxide nanocomposite: a cost-effective approach," J. Sci. Adv. Mater. Devices, **7** (1) 100391 (2022). doi:10.1016/j.jsamd.2021.08.004.
46) S. Basu, and P. Bhattacharyya, "Recent developments on graphene and graphene oxide based solid state gas sensors," Sensors Actuators B Chem., **173** 1–21 (2012). doi:10.1016/j.snb.2012.07.092.
47) V. Singh, D. Joung, L. Zhai, S. Das, S.I. Khondaker, and S. Seal, "Graphene based materials: past, present and future," Prog. Mater. Sci., **56** (8) 1178–1271 (2011). doi:10.1016/j. pmatsci.2011.03.003.
48) Y. Yao, X. Chen, H. Guo, and Z. Wu, "Graphene oxide thin film coated quartz crystal microbalance for humidity detection," Appl. Surf. Sci., **257** (17) 7778–7782 (2011). doi:10.1016/j.apsusc. 2011.04.028.
49) S. Zheng, Y. Yang, X. Li, H. Liu, W. Yan, R. Sui, and Q. Lu, "Temperature and emissivity measurements from combustion of pine wood, rice husk and fir wood using flame emission spectrum," Fuel Process. Technol., **204** 106423 (2020). doi:10.1016/j.fuproc.2020.106423.